




The Roles of the Two-Component System, MtrAB, in Response to Diverse Cell Envelope Stresses in *Dietzia* sp. DQ12-45-1b

Xiaoyu Qin,^a Kaiduan Zhang,^a Yong Nie,^a  Xiao-Lei Wu^{a,b,c}

^aCollege of Engineering, Peking University, Beijing, China

^bInstitute of Ocean Research, Peking University, Beijing, China

^cInstitute of Ecology, Peking University, Beijing, China

ABSTRACT Two-component systems (TCSs) act as common regulatory systems allowing bacteria to detect and respond to multiple environmental stimuli, including cell envelope stress. The MtrAB TCS of Actinobacteria is critical for cell wall homeostasis, cell proliferation, osmoprotection, and antibiotic resistance, and thus is found to be highly conserved across this phylum. However, how precisely the MtrAB TCS regulates cellular homeostasis in response to environmental stress remains unclear. Here, we show that the MtrAB TCS plays an important role in the tolerance to different types of cell envelope stresses, including environmental stresses (i.e., oxidative stress, lysozyme, SDS, osmotic pressure, and alkaline pH stresses) and envelope-targeting antibiotics (i.e., isoniazid, ethambutol, glycopeptide, and β -lactam antibiotics) in *Dietzia* sp. DQ12-45-1b. An *mtrAB* mutant strain exhibited slower growth compared to the wild-type strain and was characterized by abnormal cell shapes when exposed to various environmental stresses. Moreover, deletion of *mtrAB* resulted in decreased resistance to isoniazid, ethambutol, and β -lactam antibiotics. Further, Cleavage under targets and tagmentation sequencing (CUT&Tag-seq) and electrophoretic mobility shift assays (EMSAs) revealed that MtrA binds the promoters of genes involved in peptidoglycan biosynthesis (*IdtB*, *IdtA*, *murJ*), hydrolysis (GJR88_03483, GJR88_4713), and cell division (*ftsE*). Together, our findings demonstrated that the MtrAB TCS is essential for the survival of *Dietzia* sp. DQ12-45-1b under various cell envelope stresses, primarily by controlling multiple downstream cellular pathways. Our work suggests that TCSs act as global sensors and regulators in maintaining cellular homeostasis, such as during episodes of various environmental stresses. The present study should shed light on the understanding of mechanisms for bacterial adaptivity to extreme environments.

IMPORTANCE The multilayered cell envelope is the first line of bacterial defense against various extreme environments. Bacteria utilize a large number of sensing and regulatory systems to maintain cell envelope homeostasis under multiple stress conditions. The two-component system (TCS) is the main sensing and responding apparatus for environmental adaptation. The MtrAB TCS highly conserved in Actinobacteria is critical for cell wall homeostasis, cell proliferation, osmoprotection, and antibiotic resistance. However, how MtrAB works with regard to signals impacting changes to the cell envelope is not fully understood. Here, we found that in the Actinobacterium *Dietzia* sp. DQ12-45-1b, a TCS named MtrAB is pivotal for ensuring normal cell growth as well as maintaining proper cell morphology in response to various cell envelope stresses, namely, by regulating the expression of cell envelope-related genes. Our findings should greatly advance our understanding of the adaptive mechanisms responsible for maintaining cell integrity in times of sustained environmental shocks.

KEYWORDS *Dietzia* sp. DQ12-45-1b, two-component system, MtrAB, stress, response, antibiotic resistance, cell morphology

Editor Ning-Yi Zhou, Shanghai Jiao Tong University

Copyright © 2022 Qin et al. This is an open-access article distributed under the terms of the [Creative Commons Attribution 4.0 International license](https://creativecommons.org/licenses/by/4.0/).

Address correspondence to Yong Nie, nieyong@pku.edu.cn, or Xiao-Lei Wu, xiaolei_wu@pku.edu.cn.

The authors declare no conflict of interest.

Received 9 August 2022

Accepted 30 August 2022

Published 3 October 2022

Microorganisms inhabit diverse environments, often enduring conditions too extreme for other life forms to exist. The adaptive responses of microorganisms to environmental conditions lay the foundations for microbial life and its function in the global geobiochemical cycle, its use in bioremediation, and bioindustry, as well as its role in pathogenesis.

The cell envelope constitutes the first line of defense against life-threatening external stress. The roles of the cell envelope include keeping the integrity of the cell, selectively transporting nutrients and waste products, maintaining cellular homeostasis, and protecting the cell from harmful environmental conditions. The envelope of Gram-negative bacteria is composed of an outer membrane, a periplasm containing a peptidoglycan layer, and an inner membrane. In contrast, the cell envelope of Gram-positive bacteria consists of 2 functional layers; a cytoplasmic membrane, and a cell wall, except for the order *Corynebacteriales*. Compared with other Gram-positive bacteria, species from the order *Corynebacteriales*, which includes the important pathogen *Mycobacterium*, the production strain *Corynebacterium*, and the environmental strain *Dietzia*, are characterized by a more complex multi-layered cell envelope. These species possess an additional polysaccharide layer consisting of arabinogalactan and an outer membrane layer composed of mycolic acids (1, 2).

Certain stresses can disturb the integrity of the cell envelope, and therefore threaten the survival of the cell. Such stresses are referred to as cell envelope stresses and they include environmental types of stresses (e.g., temperature shocks, changing pH, osmotic stress, oxidative stress, and envelope-targeting antibiotics) as well as cell-intrinsic types of stresses (e.g., protein misfolding, mutation, secretion defects, and membrane disruption) (3, 4). Thus, the survival of microorganisms critically depends on their ability to sense envelope stresses, activate stress responses, and ultimately restore envelope homeostasis.

To respond to cell envelope stresses in a timely and proportionate manner, microorganisms have developed various defense systems. One of the best-known regulatory systems responsible for cell envelope stress sensing and response are so-called two-component systems (TCSs) (3). Prototypical TCSs typically consist of a histidine kinase (HK) serving as a stress sensor and a response regulator (RR) serving as a regulatory effector. The cell envelope stress-responsive TCSs can be activated by cell envelope stress signals, such as the integrity of the cell envelope (3, 5, 6). These activated TCSs commonly serve as global regulators to maintain cellular homeostasis. One example of such TCSs is the CpxAR identified earlier in *Escherichia coli*. The CpxAR TCS consists of a histidine kinase CpxA and a regulatory protein CpxR. This system is activated by signals that negatively affect the functioning of the cell envelope such as alkaline pH, overexpression of specific envelope protein, high osmolarity, and perturbations in membrane structure (4, 7, 8). The regulon of the CpxAR TCS consists of more than 100 different genes, many of which encode factors in protein folding and degradation, and proteins involved in efflux, biofilm formation, and antibiotic resistance (9, 10). Another example of cell envelope stress-responsive TCSs is the non-orthodox Rcs TCS found in Enterobacteriaceae. This TCS was shown to be activated via the outer membrane or peptidoglycan perturbation, lipopolysaccharide (LPS) synthesis defects, lipoprotein mislocalization, osmotic and oxidative stress, and β -lactam antibiotics. The Rcs TCS subsequently regulates downstream genes involved in virulence, capsule biosynthesis, biofilm formation, and motility (11–13).

While a considerable number of cell envelope stress-responsive TCSs have been described, few studies have so far focused on TCSs that regulate cell envelope homeostasis directly in response to stresses targeting the cell envelope. For example, the WalkR TCS, which is highly conserved in low G+C Gram-positive bacteria, was found to be induced by antibiotics targeting the late stages of peptidoglycan synthesis. The WalkR regulon includes a large number of genes that participate in cell wall biosynthesis, metabolism, and cell division (14, 15). In *Vibrio cholerae*, the WigKR TCS controls cell envelope homeostasis in response to cell wall stress induced by various antibiotics (16). Notably, similar cell envelope stress response systems have not been reported in *Corynebacteriales*, which are characterized by the cell envelope of complex composition.

The MtrAB TCS, which is conserved in Actinobacteria, plays multiple roles in cell wall metabolism, cell division, DNA replication, and cell proliferation (17–19). In *Mycobacterium tuberculosis*, MtrA expression is downregulated when cells encounter envelope stresses such as SDS and DETA-NO (17). Importantly, *M. tuberculosis* requires MtrB to withstand acid stress (pH 5.5) and hypoxia (20). Moreover, the MtrAB TCS plays a critical role in the osmoregulation and susceptibility to cell wall-targeting antibiotics in *Corynebacterium glutamicum* (21). Together, these findings suggested that the MtrAB TCS is important for the response to specific envelope stresses. However, which cell envelope stress responses are related to MtrAB has remained unclear. Previous studies using *M. tuberculosis* reported that its MtrA directly regulates cell envelope homeostasis via peptidoglycan synthetase genes *ftsI*, *dacB1*, *wag31*, peptidoglycan hydrolase genes *ripA*, *rpfa-E*, and genes involved in mycolic acids assembly (*fbpB*, *fbpC*) (17). MtrB can interact with peptidoglycan synthetase FtsI, Wag31, and cell envelope biosynthesis regulators PknA and PknB (22). In comparison, the peptidoglycan hydrolase genes *mepA*, *nlpC*, and *rfp2* are directly repressed by MtrA in *C. glutamicum* (23). In addition, deletion of either MtrA or MtrB in both Mycobacteria and Corynebacteria alters their cell morphology, suggesting that the MtrAB TCS affects cell envelope homeostasis (17, 21, 24). Therefore, cell envelope stress response of MtrAB and cell envelope homeostasis in Actinobacteria are possibly linked at a mechanistic level.

The actinobacterial genus *Dietzia* is widely distributed in diverse habitats, such as soda lakes (25, 26), deep seas (27, 28), the soil of deserts (29, 30), oil fields (31, 32), the surface of plants (33), and clinical samples (34–36). Several *Dietzia* strains are potential human pathogens in immunocompetent and immunocompromised patients (37–39). As most *Dietzia* species can degrade a wide range of alkanes and aromatic compounds, and they can tolerate high alkaline and salty environments (40), they have great potential for bioremediation in alkaline and salty environments (41). Moreover, *Dietzia* species have many applications in the food, medical, and chemical industries (40, 42). Interestingly, some *Dietzia* species are thought to be potential probiotics to reduce *Mycobacterium avium paratuberculosis* (MAP) (43, 44).

Here, we set out to investigate the effects of deleting *mtrAB* genes on the growth and cell morphology under the cell envelope, ultimately aiming to better understand the role of the MtrAB TCS in cell envelope stress resistance in *Dietzia* sp. DQ12-45-1b. Using CUT&Tag-seq combined with electrophoretic mobility shift assays (EMSAs), we constructed a regulatory network of MtrAB in *Dietzia* sp. DQ12-45-1b. In summary, our findings reveal that the MtrAB TCS plays a critical role in the response to a variety of cell envelope stresses and in maintaining cell envelope homeostasis.

RESULTS

Deletion of the *mtrAB* genes decreases the growth of *Dietzia* sp. DQ12-45-1b under diverse envelope stresses. Based on the phylogenetic analysis of MtrAB in *Corynebacterineae* and *Streptomycineae* suborders, we found that both MtrA and MtrB phylogenetic trees consisted of 4 distinct clusters. Sequences from the families *Dietziaceae* and *Corynebacteriaceae* of the suborder *Corynebacterineae* formed two clusters that were distinct from the sequences of other *Corynebacterineae* species (Fig. S1 and S2). The results suggested that the MtrAB TCS in the family of *Dietziaceae* has unique functions compared to other families of *Corynebacterineae* suborder. To investigate whether the MtrAB TCS of *Dietzia* sp. DQ12-45-1b is involved in bacterial adaptation to cell envelope stresses, we compared the growth of *Dietzia* sp. DQ12-45-1b and its *mtrAB* mutant strain under a number of conditions causing envelope stress. As shown in Fig. 1, the inactivation of *mtrAB* genes significantly suppressed the growth of *Dietzia* sp. DQ12-45-1b under a range of stresses, including oxidative stress, lysozyme, SDS, osmotic pressure, and alkaline stress. The *mtrAB* complementary strains exhibited similar growth to that of the wild-type strain under all culture conditions (Fig. 1). Together, these findings suggested that MtrAB TCS plays an important role in cellular resistance to diverse cell envelope-related stress conditions. Moreover, we found that all strains (i.e., the wild-type, Δ *mtrAB* mutant, and *mtrAB* complementary strains) exhibited near-

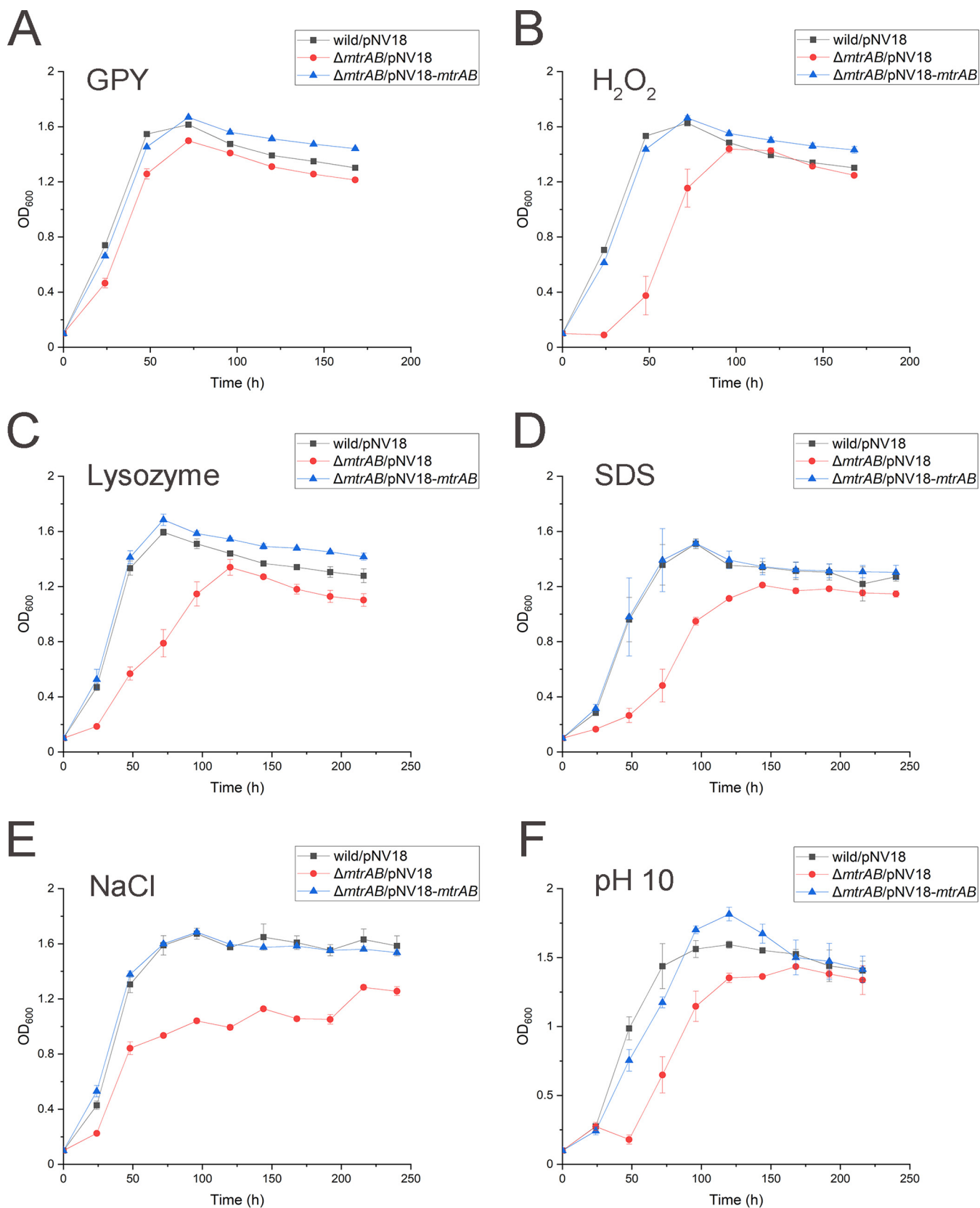


FIG 1 Growth curves of *Dietzia* sp. DQ12-45-1b wild-type strain carrying pNV18, $\Delta mtrAB$ carrying pNV18 (empty plasmid), pNV18-*mtrAB* under different stresses. (A) GPY medium; (B) GPY medium with 0.0025% H₂O₂; (C) GPY medium with 2 μ g/mL lysozyme; (D) GPY medium with 0.0005% SDS; (E) GPY medium with 0.625M NaCl; (F) pH 10 GPY medium. The results shown represent the mean values (\pm SD) of three replicates.

identical growth patterns when grown in glucose peptone yeast (GPY) medium (Fig. 1A), which is an optimal medium for *Dietzia* spp. (45). These results suggested that MtrAB remains inactive in the absence of environmental stress.

Deletion of *mtrAB* affects the susceptibility of *Dietzia* sp. DQ12-45-1b to antibiotics. To investigate the effects of deletion of MtrAB TCS in antibiotic sensitivity in *Dietzia* sp. DQ12-45-1b, we determined the minimum inhibitory concentrations (MICs) of envelope-targeting antibiotics including isoniazid, ethambutol, glycopeptide (i.e., vancomycin), and β -lactam antibiotics (i.e., ampicillin, cephalexin, and penicillin) against *Dietzia* sp. DQ12-45-1b wild-type, the $\Delta mtrAB$ mutant, as well as the complementary strains. The $\Delta mtrAB$ mutant strain showed a 2-fold decrease in the MICs of ethambutol, a 4-fold decrease in the MICs of cephalexin and penicillin, and an 8-fold decrease in the MICs of isoniazid and ampicillin compared to the wild-type strain. In comparison, the $\Delta mtrAB$ mutant strain showed a 2-fold increase in the MICs of vancomycin compared with the wild-type strain (Table 1). Together, these results suggested that MtrAB TCS contributes to establishing resistance against cell envelope-targeting antibiotics, especially antibiotics targeting mycolic acids (isoniazid) and penicillin-binding proteins (β -lactam antibiotics).

MtrAB TCS regulates peptidoglycan biosynthesis and cell division under envelope stress conditions. Together, these findings indicated that MtrAB TCS senses the extracellular stresses and maintains cellular homeostasis. To investigate how the inactivation of MtrAB affected the cellular response to cell envelope stresses, we compared transcript abundance in the wild-type and $\Delta mtrAB$ mutant strains under alkaline conditions, a typical representative of cell envelope stresses (4). As shown in Fig. 2A, 144 genes were upregulated and 253 genes were downregulated in the $\Delta mtrAB$ mutant when compared to the wild-type strain under alkaline stress conditions by the global analysis of differentially expressed genes (DEGs). Our KEGG enrichment analysis showed that 7 genes of the “peptidoglycan biosynthesis” pathway were induced in the $\Delta mtrAB$ mutant under alkaline stress (Fig. S3 and Table S1). We also found that the expression of a large number of genes involved in peptidoglycan biosynthesis (*murCDEFGJ*, *ftsW*, *ftsI*, *mraY*, *ldtA*, *ldtB*), hydrolysis (*cwIO*, *mepA*, *ripA*, GJR88_00456, GJR88_04713), cell division and elongation (*ftsEXLK*, *sepF*, *sepIVA*, *wag31*), and related regulators (*envC*, *whmD*, *mraZ*, GJR88_04446, GJR88_03645) significantly changed in the $\Delta mtrAB$ mutant compared with the wild-type strain when exposed to alkaline stress. However, at pH 8, these genes exhibited similar transcript levels in both the wild-type and $\Delta mtrAB$ mutant strains (Fig. 2B, Fig. S4, and Table S1). Together, these results were consistent with our findings, showing that the MtrAB TCS regulates cell envelope homeostasis during cell envelope stress conditions.

Inactivation of *mtrAB* alters cell morphology under cell envelope stresses. As the results in the previous section indicated that MtrAB regulates genes involved in peptidoglycan homeostasis and cell division, we next analyzed the cell shapes and measured the lengths of the wild-type, $\Delta mtrAB$ mutant, and complementary strains in response to different cell envelope stresses. Similarly, the wild-type, $\Delta mtrAB$ mutant, and complementary strains were cultured in oxidative, lysozyme, SDS, osmotic pressure, and alkaline pH stresses. When grown in GPY medium to the middle exponential phase, both the wild-type strain and the $\Delta mtrAB$ mutant exhibited short-rod shapes.

TABLE 1 MICs for different antibiotics of *Dietzia* sp. DQ12-45-1b wild/pNV18, $\Delta mtrAB$ /pNV18, and $\Delta mtrAB$ /pNV18-*mtrAB*

Antibiotics	MIC for <i>Dietzia</i> sp. DQ12-45-1b strains ($\mu\text{g/mL}$)			Fold change (WT/ Δ)
	Wild/pNV18	$\Delta mtrAB$ /pNV18	$\Delta mtrAB$ /pNV18- <i>mtrAB</i>	
Isoniazid	4096	512	4096	8
Ethambutol	8	4	2	2
Vancomycin	0.125	0.25	0.25	0.5
Ampicillin	4	0.5	2	8
Cephalexin	8	2	4	4
Penicillin	2	0.5	2	4

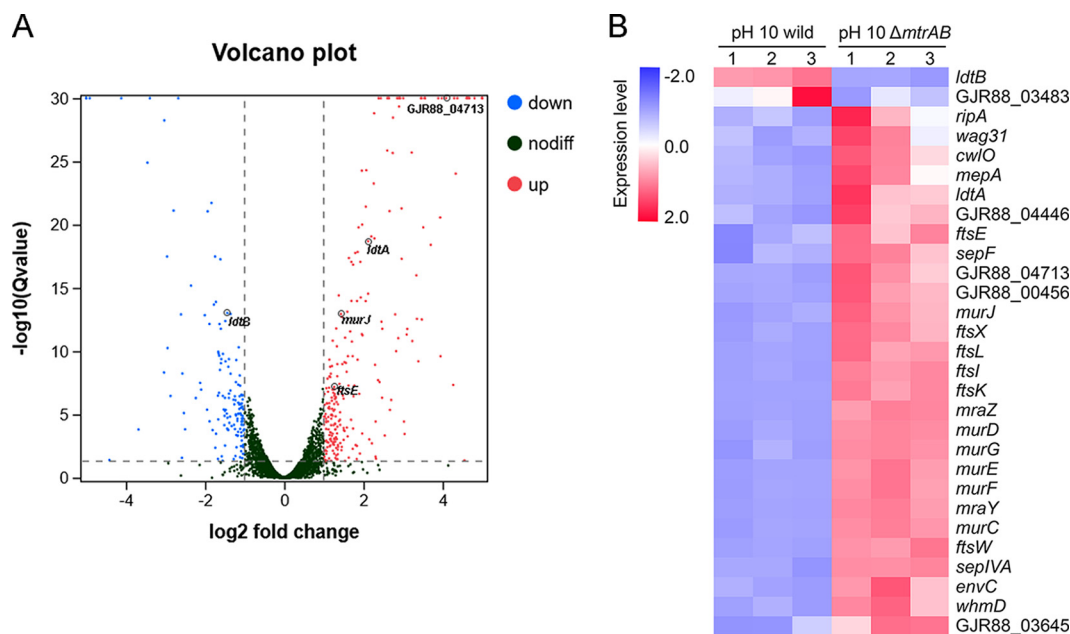


FIG 2 Comparison of transcriptional differences of *Dietzia* sp. DQ12-45-1b wild-type and $\Delta mtrAB$ mutant strains under the alkaline pH condition. (A) Volcano plot of the differentially expressed genes (DEGs). (B) Heatmap of the expression levels in DEGs involved in cell envelope homeostasis (fold change ≥ 2 , FDR ≤ 0.05). The expression data were normalized by row Z-scores using FPKM values. Red represents upregulated genes, blue represents downregulated genes.

We found that in response to oxidative, lysozyme, SDS, osmotic pressure, and alkaline pH stresses, the lengths of cells increased in the $\Delta mtrAB$ mutant strain, with the mean length of 1.15–1.59 μm for the wild-type strain and 2.31–2.75 μm for the $\Delta mtrAB$ mutant (Fig. 3A and B). In addition to increased lengths, the $\Delta mtrAB$ mutant cells showed irregular and branched shapes in response to cell envelope stresses (Fig. 3A). The complementary strain can restore these phenotypes of cell morphology. Together, these results confirmed that the MtrAB TCS regulates peptidoglycan metabolism and cell division to maintain cellular homeostasis in response to cell envelope stress conditions.

Identification of candidate genes regulated by the regulator MtrA. To investigate whether the MtrAB TCS directly regulates these genes, we defined the MtrA regulon in *Dietzia* sp. DQ12-45-1b using the Cleavage Under Targets and Tagmentation (CUT&Tag) technology (46). A previous study reported that glutamic acid replacement at a residue corresponding to D56 of MtrA creates a constitutively active MtrA (47). Based on this finding, we generated the MtrA (D56E) mutant and overexpressed this mutant in *Dietzia* sp. DQ12-45-1b wild-type strain for CUT&Tag assay. We analyzed the sequences of the binding regions derived from CUT&Tag data using MEME (48). As shown in Fig. 4A, a 21-nucleotide consensus motif with seven imperfect TCG appears to be essential for MtrA binding (Fig. 4A).

Based on these CUT&Tag data, we further identified an additional 103 DNA-binding genes (Table S2), including 6 genes involved in peptidoglycan biosynthesis (transpeptidase genes *ldtB*, *ldtA*, and flippase gene *murJ*), hydrolysis (hydrolase genes GJR88_03483, GJR88_4713), and cell division (cell division gene *ftsE*). The upstream regions of all these genes contained the TCG-rich consensus motif (Table 2). Moreover, the expression of 5 genes (*ldtB*, *ldtA*, *murJ*, *ftsE*, GJR88_4713) significantly changed in the $\Delta mtrAB$ mutant compared with the wild-type strain in response to alkaline stresses. In addition, the hydrolase gene GJR88_03483 was downregulated in the $\Delta mtrAB$ mutant compared to the wild-type strain in pH 8 conditions (Fig. 2, Fig. S4, and Table S1). The transcription levels of these genes were then verified by quantitative reverse transcription-PCR (qRT-PCR) (Fig. S5). We next tested whether MtrA binds to the upstream regions of the above 6 genes using EMSA analysis. As shown in Fig. 4C, MtrA bound to these regions *in vitro* (Fig. 4B). In

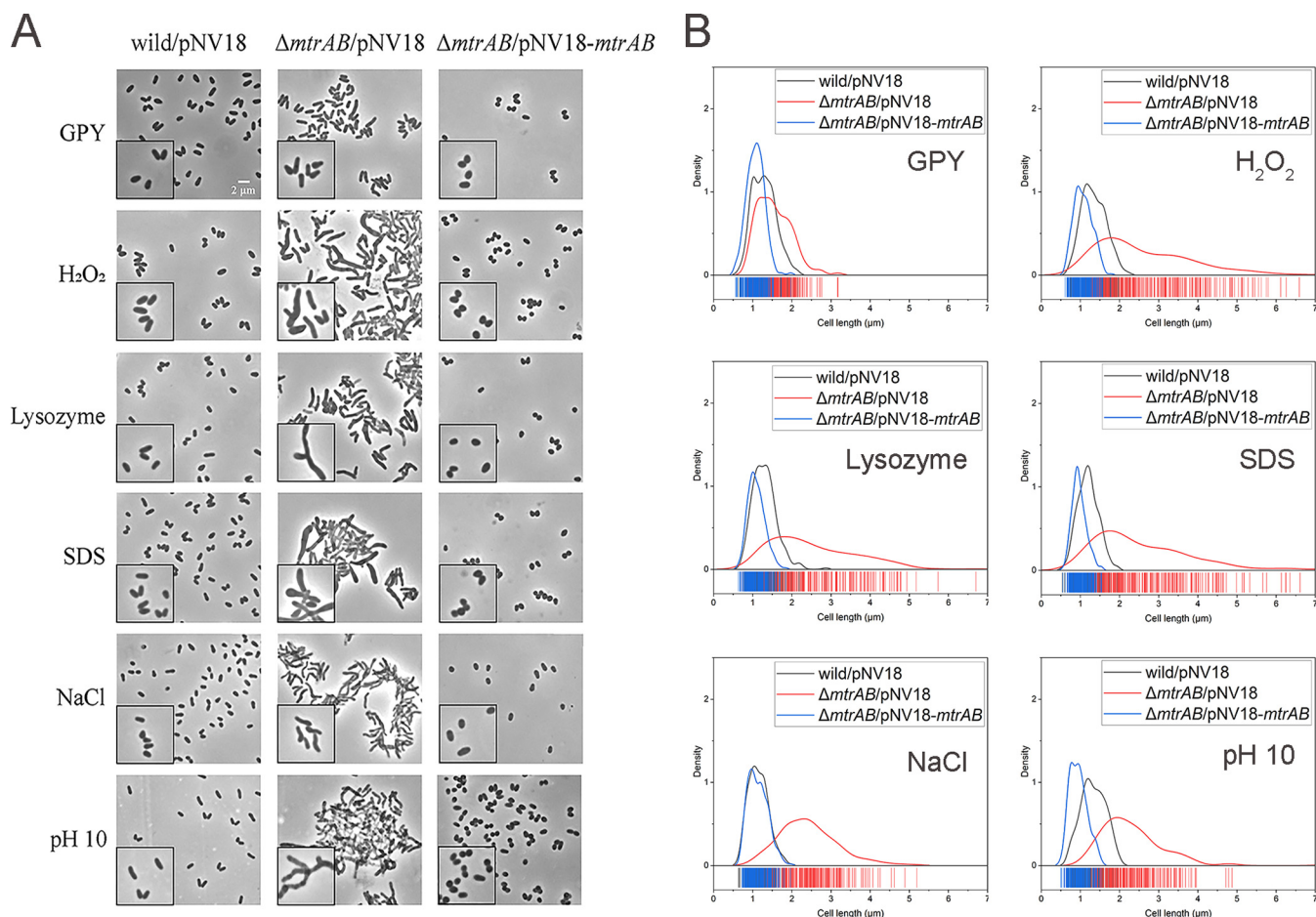


FIG 3 Cell morphology of *Dietzia* sp. DQ12-45-1b wild-type strain carrying pNV18, $\Delta mtrAB$ carrying pNV18 (empty plasmid), pNV18-*mtrAB* under different stresses. (A) The representative micrographs of the wild/pNV18, $\Delta mtrAB$ /pNV18, and $\Delta mtrAB$ /pNV18-*mtrAB* under various conditions. Inserts show a small portion of each image. (B) Distribution curves of the cell lengths of ~ 200 cells/sample from (A) were measured using the Digimizer software.

addition, MtrA failed to bind to the negative control DNA (Fig. 4B). Together, these results demonstrated that MtrA directly represses the expression of *ldtA*, *murJ*, *ftsE*, and GJR88_04713 genes, and activates the *ldtB* and GJR88_03483 genes (Fig. 4C). Critically, the uncontrolled activity of synthetases and hydrolases can lead to an imbalance between peptidoglycan synthesis and degradation, leading to cell deformation and lysis (49, 50). In addition, it has been reported that FtsE promotes divisome assembly and regulates septal peptidoglycan splitting (51). Therefore, MtrA presumably serves both activator and repressor functions critical for maintaining cell envelope homeostasis in *Dietzia* sp. DQ12-45-1b, especially in response to cell envelope stress conditions.

DISCUSSION

Here, we demonstrated that the two-component system MtrAB is critical for maintaining normal survival and cell envelope homeostasis in response to various cell envelope stress conditions, such as oxidative, SDS, alkaline, and cell envelope-targeting antibiotic stresses. Through RNA-Seq, CUT&Tag-Seq and EMSA analysis, we found that MtrA directly represses peptidoglycan-related transpeptidase gene *ldtA*, flippase gene *murJ*, hydrolase gene GJR88_04713, cell division gene *ftsE*, and activates transpeptidase gene *ldtB* and hydrolase gene GJR88_03483 in *Dietzia* sp. DQ12-45-1b.

Previous studies have reported that the MtrAB TCS affects tolerance to many antibiotics targeting cell envelope. In *Mycobacterium smegmatis*, the $\Delta mtrA$ mutant was found to be more resistant to isoniazid, but more sensitive to vancomycin and rifampin than the parent strain, and showed a modest increase in sensitivity to ampicillin (17).

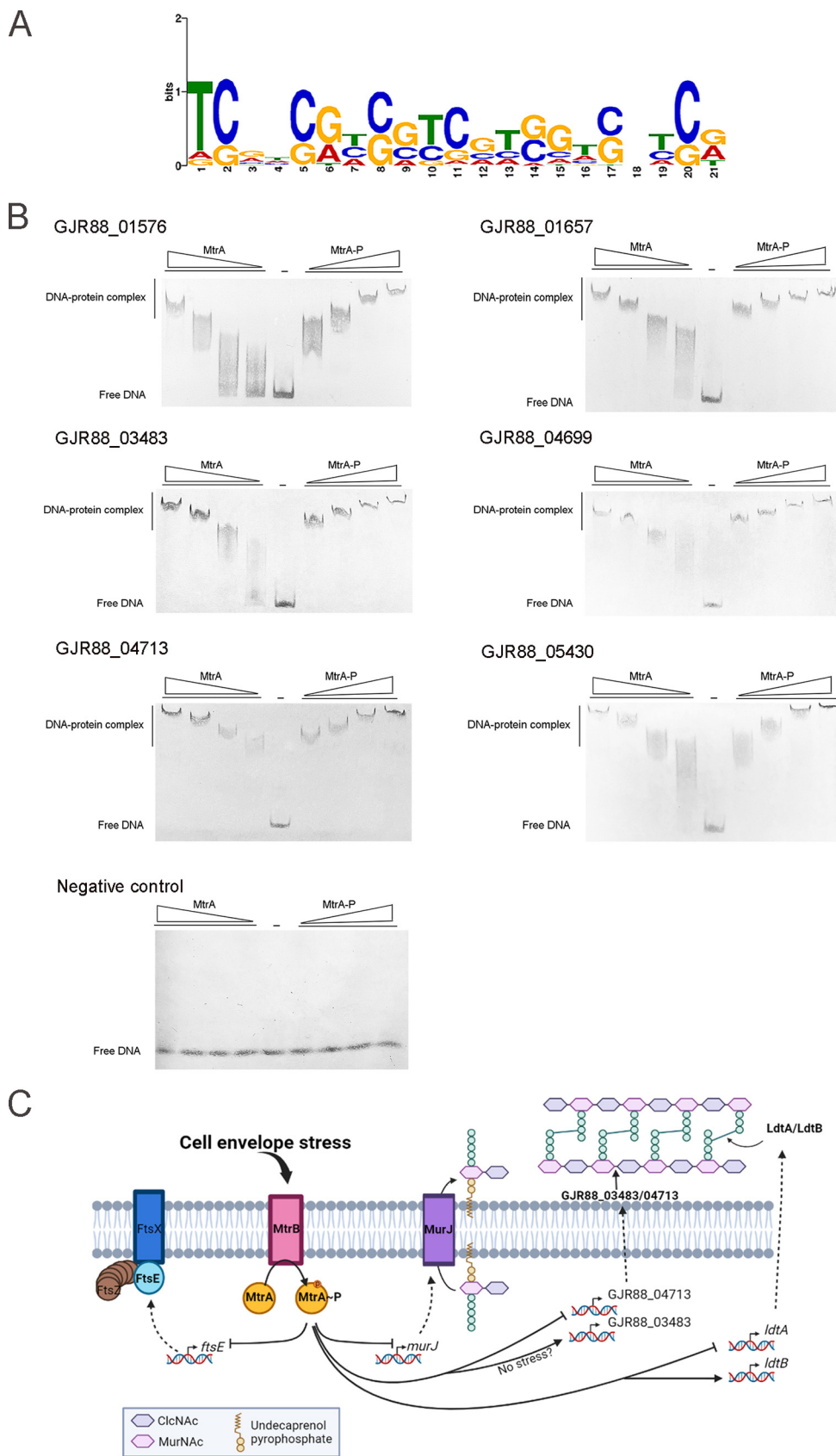


FIG 4 Identification and validation of MtrA motif and analysis of predicted MtrA sites upstream of the genes involved in peptidoglycan homeostasis in *Dietzia* sp. DQ12-45-1b. (A) Predicted consensus MtrA binding site (Continued on next page)

TABLE 2 The probes for the MtrA site of the six selected promoters^a

Gene ID	Sequence (5'→3')	Product	Gene name
GJR88_01576	GTCGGCGCGGTCGGCGTGGTCGTCGTCGGCACGCGTCGTCCC	Cell division ATP-binding protein	<i>ftsE</i>
GJR88_01657	CTGGCTCAGTTCATGGTCGGAAGGGACATGACGCTCGGAAG	Putative L,D-transpeptidase	<i>ldtB</i>
GJR88_03483	GCGTGGGTGATCGTGATGGCGGTGGAGAACGTCGGCCGTGCG	Membrane-bound lytic murein transglycosylase B	NA ^b
GJR88_04699	ACTGCCGACACACCGCGCCACGGGTTCTGTACGTATG	L,D-transpeptidase family protein	<i>ldtA</i>
GJR88_04713	TCACAATTCGTCGGTGTGCGACAACCGGCGGTGGTGGTGT	Lysozyme M1 (1,4-beta-N-acetylmuramidase)	NA
GJR88_05430	CTCGCCGCGGTTCATCACCTCGTGGTCACCGTCTGATCCT	Flippase	<i>murJ</i> , <i>mviN</i>

^aThe underlined letters of sequences represent the predicted MtrA-binding sites.

^bNA, gene name was not assigned.

In *C. glutamicum*, the $\Delta mtrAB$ mutant was more sensitive to penicillin, vancomycin, and lysozyme, but more resistant to ethambutol compared to the wild-type strain (21). In our study, the $\Delta mtrAB$ mutant showed significantly higher resistance to vancomycin and decreased resistance to isoniazid, ethambutol, ampicillin, cephalexin, and penicillin compared to *Dietzia* sp. DQ12-45-1b wild-type strain. Isoniazid targets InhA which is a long-chain enoyl-acyl carrier protein reductase essential for the biosynthesis of mycolic acid (52). Ethambutol perturbs the cell wall arabinogalactan biosynthesis (53), while β -lactam antibiotics (i.e., ampicillin, cephalexin, and penicillin) are inhibitors of penicillin-binding proteins (PBPs) (54, 55). Together, these results strongly suggest that the MtrAB TCS plays a critical role in resistance to various antibiotics targeting peptidoglycan in Corynebacterineae. However, we found that the $\Delta mtrAB$ mutant of *Dietzia* sp. DQ12-45-1b was more resistant to vancomycin. This result differs from earlier findings for *M. smegmatis* and *C. glutamicum*. We hypothesize that the resistance to vancomycin of the $\Delta mtrAB$ mutant in *Dietzia* sp. DQ12-45-1b is caused by the diversity of different bacterial species (Fig. S1 and S2). In addition, vancomycin relies on binding to d-Ala-d-Ala to inhibit the biosynthesis of peptidoglycan (56). d-Ala-d-Ala in the peptidoglycan layers which remain unprocessed by PBPs and the murein monomers in the cytoplasmic membrane are 2 established binding targets for vancomycin. To inhibit nascent peptidoglycan synthesis, vancomycin needs to pass through peptidoglycan layers before binding to murein monomers. As a result, many vancomycin molecules are trapped in the peptidoglycan layers. Previous studies have reported that the thickened cell envelope, the increased non-amidated mucopeptide components, and the reduced cross-linking of peptidoglycan contributed to vancomycin resistance in *Staphylococcus aureus* (VRSA) (57, 58). In *Dietzia* sp. DQ12-45-1b, cell envelope thickness of the $\Delta mtrAB$ mutant strain was thinner than the wild-type strain under optimal pH conditions (Fig. S6). Based on these findings, we speculate that the $\Delta mtrAB$ mutant of *Dietzia* sp. DQ12-45-1b possesses a larger number of PBPs unprocessed peptidoglycan or non-amidated mucopeptides than wild-type strain to trap more vancomycin molecules. As a result, the $\Delta mtrAB$ mutant strain exhibits reduced susceptibility to vancomycin. This speculation can be studied in future research. Moreover, our $\Delta mtrAB$ mutant showed decreased resistance to isoniazid, ethambutol, and β -lactam antibiotics, which further provided evidence for the role of the MtrAB TCS in cell envelope synthesis and metabolism and even the biosynthesis of mycolic acid and arabinogalactan.

It has been reported that peptidoglycan synthetase genes *ftsI*, *dacB1*, *wag31*, and hydrolase genes *ripA*, *rfpA-E* are directly regulated by MtrA in *M. tuberculosis* (17). Moreover, in *C. glutamicum*, MtrA directly represses peptidoglycan hydrolase genes *mepA*, *nlpC*, and *rfp2* (23). In our study, we showed that in *Dietzia* sp. DQ12-45-1b, MtrA directly activates peptidoglycan hydrolase gene GJR88_03483, transpeptidase gene

FIG 4 Legend (Continued)

generated from MEME analysis based on CUT&Tag data (48). The *E*-value of the motif is 4.2e-029. The height of each nucleotide represents the relative frequency. (B) EMSA analysis of MtrA binding to the six selected promoters and nonspecific DNA (*Escherichia coli* DNA fragment). The reactions were performed at different concentrations of MtrA and MtrA-P (0, 0.5, 1, 2.5, and 5 μ M). The nonspecific DNA was used as a negative control. (C) Proposed model of MtrA regulatory network on the genes that governed peptidoglycan synthesis and hydrolysis.

ldtB, and represses peptidoglycan hydrolase gene GJR88_04713, transpeptidase gene *ldtA*, flippase gene *murJ*, cell division gene *ftsE*. The phylogenetic analysis showed that the MtrA proteins from *M. tuberculosis*, *C. glutamicum*, and *Dietzia* sp. DQ12-45-1b are distributed in different clusters in the phylogenetic tree (Fig. S1), which might explain the variations in the genes that MtrA regulated among these strains. These results also suggested that the MtrAB TCS has more diverse functions than what we have revealed.

Many TCSs are involved in sensing signals and regulating adaptive genes for stress tolerance; however, the precise molecular nature of the specific signal involved remains unknown. The specific inductive signals of histidine kinases may correlate with regulatory pathways of response regulators occasionally. For example, the signals for the CpxAR TCS are thought to be secreted, misfolded proteins in the periplasm, with its regulon consisting of genes that encoded protein folding and degradation factors (4, 9, 10, 59). The RcsBCDF system senses lipopolysaccharide (LPS) defects or cell envelope damage, which then causes changes in the expression of genes involved in virulence and capsule biosynthesis (11–13, 60–62). The signal for the WalkR TCS is thought to be the level and/or availability of Lipid II outside the cytoplasmic membrane, with its regulon containing genes involved in cell envelope homeostasis (14, 63). However, the signals which activate the MtrAB TCS in Actinobacteria were unclear. In our study, in *Dietzia* sp. DQ12-45-1b, we found that the MtrAB TCS plays an important role under various cell envelope stresses; as a result, inductive signals for the MtrB sensor presumably were components triggered by multiple stresses such as peptidoglycan fragments. Interestingly, previous studies have reported that peptidoglycan fragments might act as a signaling molecule of Ser/Thr protein kinases (64–66). The signal-induced MtrB may quickly activate MtrA to regulate downstream genes involved in cell division and cell envelope homeostasis. Future research should focus on identifying the precise signals recognized by MtrAB TCS and how MtrB is activated.

Certain peptidoglycan enzymes with overlapping activity can be preferentially used for survival under specific environmental conditions. For example, in *Escherichia coli*, PBP1a synthetase and MltG hydrolase are required for survival at alkaline pH stress, in addition, PBP1b synthetase and MltA hydrolase are needed under acidic pH (67, 68). In *Dietzia* sp. DQ12-45-1b, both GJR88_03483, and GJR88_04713 directly regulated by MtrA are annotated as peptidoglycan hydrolases with lysozyme activity. This activity allows the cutting of the β -1-4 glycosidic bond between N-acetylmuramic acid and N-acetylglucosamine residues (69). Our transcriptome analysis showed that only GJR88_04713 was downregulated in the wild-type strain, but was upregulated in the Δ *mtrAB* mutant at pH 10. However, GJR88_03483 was repressed in the Δ *mtrAB* mutant at optimal pH (pH 8). Therefore, we speculate that GJR88_03483 plays a critical role in pH 8. In addition, GJR88_04713 was required at alkaline pH in *Dietzia* sp. DQ12-45-1b. Except for the different expression levels of GJR88_04713 and GJR88_03483 genes, we also found that in *Dietzia* sp. DQ12-45-1b, *LdtA* was repressed under alkaline stress, while *LdtB* was directly activated by MtrA. Previous studies reported that 3–3 cross-links between muropeptides were produced by LD-transpeptidases (LDTs) in bacteria (70, 71). In addition, LDTs can catalyze the formation of the linkage between the Braun lipoprotein (Lpp) and muropeptide in *E. coli* (72). Multiple functions of LDTs suggested that *LdtA* and *LdtB* may contain extra functions in addition to forming the 3–3 cross-links in *Dietzia* sp. DQ12-45-1b in alkaline stress.

In summary, our study provides compelling evidence that in *Dietzia* sp. DQ12-45-1b, the MtrAB TCS fulfills an important role in response to cell envelope stresses and maintaining cell envelope homeostasis, namely, by directly regulating genes involved in peptidoglycan homeostasis and cell division. Because this cell envelope stress sensing and response system might be common in Actinobacteria, our study provides critical insights into the industrial production of applied bacteria and virulence regulation of pathogens. Our findings strongly suggest that TCSs act both as a general sensor as well as a global regulator in maintaining cellular homeostasis, especially during times of harsh environmental conditions. The findings provide novel insights into the

understanding of mechanisms for microbial adaptation to diverse environmental stress conditions.

MATERIALS AND METHODS

Bacterial strains and growth conditions. The strains and plasmids used in this study are shown in Table 3.

Dietzia sp. DQ12-45-1b wild-type, mutant, and complementary strains were cultured in GPY medium (10 g/L glucose, 10 g/L tryptone, and 5 g/L yeast extract) with the appropriate antibiotics (streptomycin 30 μ g/mL, and kanamycin 50 μ g/mL) at 30°C and shaken at 150 rpm. *E. coli* DH5 α and its recombinants were grown in LB medium (10 g/L NaCl, 10 g/L tryptone, and 5 g/L yeast extract) at 37°C with shaking at 150 rpm.

For all growth experiments for *Dietzia* sp. DQ12-45-1b strains under different stress conditions, 96-well plates were used at 30°C with shaking at 600 rpm. Growth curves were monitored at intervals of 24 h via a microplate reader (SpectraMax i3, Molecular Devices) at 600 nm. All the cultures were normalized OD₆₀₀ to 0.1 and were allowed to grow in GPY medium with different stresses. For oxidative, lysozyme, and SDS stress experiments, either 2 μ L of 2.5% H₂O₂, or 2 mg/mL lysozyme, or 0.5% SDS was added to 200 μ L fresh GPY medium, respectively. For osmotic stress experiments, GPY medium containing 5 M NaCl was diluted to a final concentration of 0.625 M by adding fresh GPY medium. For the alkaline pH stress experiment, GPY medium was added with a mixture of 0.2 M Na₂CO₃ and 0.2 M NaHCO₃ to pH 10. All growth curve experiments were performed in 3 biological replicates.

Phylogenetic analysis. The amino acid sequences of MtrA and MtrB were obtained from the UniProtKB and NCBI's non-redundant protein (NR) databases (Table S1). The sequences were aligned using the ClustalW (73). Phylogenetic trees were generated using the neighbor-joining method (74) by MEGA software using the default parameters (75).

Construction of Δ mtrAB mutant and complementary strains. To prepare the electrocompetent cells of *Dietzia* sp. DQ12-45-1b wild/pJV53 (76, 77), *Dietzia* sp. DQ12-45-1b wild/pJV53 was cultured in GPY medium at OD₆₀₀ of 0.05 in the presence of kanamycin (50 μ g/mL) and 0.5% glycine overnight at 30°C with shaking at 150 rpm. When grown to OD₆₀₀ of 0.4–0.6, the cultures were added with 0.2% acetamide, 0.2% Tween 80, isoniazid (0.8 mg/mL), and penicillin (0.5 μ g/mL). After 4 h of growth at 30°C, cells were harvested and washed twice with 10% glycerin by centrifugation at 1,500g (Eppendorf Centrifuge 5810 R, rotor F-34-6-38) for 10 min at 4°C. The electrocompetent cells were resuspended in 10% glycerin to achieve a final OD₆₀₀ of 50–100, and stored at –80°C for further experiments.

To generate the Δ mtrAB mutant strain, we used the double homologous recombination method (77). The upstream and downstream homologous regions of *mtrAB* (~500 bp) were amplified by PCR from the genomic DNA of *Dietzia* sp. DQ12-45-1b using the primers LF/LR and RF/RR, respectively (Table 4). The primers smF and smR were used to amplify the Sm' cassette via PCR. The DNA substrate for the replacement of the *mtrAB* gene was generated by cloning upstream and downstream homologous fragments of *mtrAB* flanking the Sm' cassette using the primers fuF and fuR via fusion PCR (Table 4). The fusion fragment was electroporated into *Dietzia* sp. DQ12-45-1b wild/pJV53 competent cells (78) (Fig. S7). Δ mtrAB mutant strain was examined by PCR using the primers idF and idR (Table 4).

For complementary vector construction, the DNA fragment of *mtrA* and *mtrB* genes was cloned from *Dietzia* sp. DQ12-45-1b genomic DNA using the primers comF and comR, both of which contained the HindIII restriction sites. Simultaneously, a DNA fragment containing p45 promoter and HindIII restriction sites was amplified from the pNV18-DsRed plasmid using the primers pF and pR by PCR (Table 4). The HindIII-digested DNA fragment of *mtrAB* was ligated into the HindIII-digested linear fragment from pNV18-DsRed without the *dsRed* gene. To obtain the complementary strain, the recombinant plasmid pNV18-*mtrAB* was electroporated into *Dietzia* sp. DQ12-45-1b Δ mtrAB mutant electrocompetent cells.

Construction of *mtrA* phosphorylation-mimic vector. The D56E mutation at the phosphorylation site in response regulator MtrA which mimics the aspartate-phosphoryl state and bypassed the requirements for MtrB sensor kinase has been already verified (47). The complete *mtrA* gene was amplified from the genomic DNA of *Dietzia* sp. DQ12-45-1b using the primers mtrAF and mtrAR with the HindIII restriction sites on both sides. The DNA fragment of the vector pNV18 was amplified with the HindIII restriction sites using the primers pNVF and pNVR from the pNV18-DsRed plasmid (Table 4). Next, the HindIII-digested DNA fragment of *mtrA* was ligated into the plasmid fragment to obtain plasmid pNV18-*mtrA*. Then the primers mtrAD56EF, mtrAD56ER, and pNVD56EF, pNVD56ER were used to amplify by PCR from pNV18-*mtrA* plasmid to replace the aspartic acid at the 56th codon with glutamate to create plasmid pNV18-*mtrA*_{D56E} using the HiEff Clone Plus One Step Cloning Kit (Yeasen). The recombinant plasmid pNV18-*mtrA*_{D56E} was electroporated into *Dietzia* sp. DQ12-45-1b wild competent cells.

Antibiotics susceptibility tests. The micro-broth dilution method was used to determine the MICs of the various antibiotics for *Dietzia* sp. DQ12-45-1b strains in 96-well plates (79). Serial 2-fold dilutions of tested antibiotics were done in the GPY medium with kanamycin (50 μ g/mL). When grown to the middle exponential phase, cells were harvested, and the pellets were washed twice with PBS buffer (pH 7.4) by centrifugation at 5,000 rpm (Eppendorf Centrifuge 5417 R, rotor FA-45-24-11) for 5 min at 4°C. All the cultures were normalized OD₆₀₀ to 0.05 with different antibiotic stresses per well at 30°C with shaking at 600 rpm for 24 h. Cultures without antibiotic stress were regarded as control. The concentration of antibiotics at which bacterial growth was inhibited by 90% compared to the control wells was MIC we tested.

Bright-field microscopy. For cell morphologic observation, cells were collected and washed three times by PBS buffer (pH 7.4) by centrifugation at 5,000 rpm (Eppendorf Centrifuge 5417 R, rotor FA-45-24-11) for 5 min at 4°C. The microscopy images were examined under a 100 \times oil immersion lens with a

TABLE 3 Strains and plasmids used in this study

Strain or plasmid	Genotype and description	Source and reference
Strains		
<i>Dietzia</i> sp. DQ12-45-1b (CGMCC 1.10709)	Wild-type	(32)
DQ12-45-1b/pNV18	Wild-type harboring pNV18; Km ^r	This study
DQ12-45-1bΔ <i>mtrAB</i>	DQ12-45-1b <i>mtrAB</i> deletion mutant; Sm ^r	This study
DQ12-45-1bΔ <i>mtrAB</i> /pNV18	DQ12-45-1b <i>mtrAB</i> deletion mutant harboring pNV18; Km ^r and Sm ^r	This study
DQ12-45-1bΔ <i>mtrAB</i> /pNV18- <i>mtrAB</i>	DQ12-45-1bΔ <i>mtrAB</i> harboring pNV18- <i>mtrAB</i> ; Km ^r and Sm ^r	This study
DQ12-45-1b wild/pNV18- <i>mtrA</i> _{D56E}	DQ12-45-1b wild-type harboring pNV18- <i>mtrA</i> _{D56E} ; Km ^r	This study
<i>E. coli</i> DH5α	Cloning strain	TransGen Biotech, China
Plasmids		
pJV53	<i>Dietzia-E.coli</i> shuttle vector (acetamide-inducible promoter); Km ^r	(77)
pNV18-DsRed	<i>Dietzia-E.coli</i> shuttle vector (p45 promoter); Km ^r	(45)
pNV18	Cloned from pNV18-DsRed.T4 without DsRed; Km ^r	This study
pNV18- <i>mtrAB</i>	pNV18 + <i>mtrA</i> and <i>mtrB</i> from DQ12-45-1b; Km ^r	This study
pNV18- <i>mtrA</i>	pNV18 + <i>mtrA</i> from DQ12-45-1b; Km ^r	This study
pNV18- <i>mtrA</i> _{D56E}	pNV18 + <i>mtrA</i> (phosphorylation-mimic) from DQ12-45-1b; Km ^r	This study

bright-field microscope. The cell length quantitative measurement uses the software Digimizer, MedCalc Ltd (80). An unpaired *t* test was used for statistical analysis.

CUT&Tag-Seq. CUT&Tag assay was performed in Ruiyuan Biotechnology Co., Ltd. (Nanjing, China). Cells overexpressing MtrA_{D56E} were grown to the middle exponential phase and then collected by centrifugation at 5,000 rpm (Eppendorf Centrifuge 5417 R, rotor FA-45-24-11) for 10 min at 4°C. The cells were digested at 37°C using 100 mg/mL lysozyme for 24 h, then collected by centrifugation at 5,000 rpm (Eppendorf Centrifuge 5417 R, rotor FA-45-24-11) for 10 min at 4°C. For CUT&Tag and library amplification, Hyperactive In-Situ ChIP Library Prep Kit for Illumina (TD901, Vazyme) was performed according to the manufacturer's instructions. Briefly, cells were incubated with 10 μL pre-treated ConA beads at room temperature for 10 min. Next, 50 μL pre-cooled antibody buffer with 0.5 μg His-tag antibody was added to the collected reaction solution for incubation at room temperature for 2 h. After primary antibody incubation, the collected reaction solution was incubated with 50 μL dig-wash buffer with 0.5 μg secondary antibody at room temperature for 1 h. Next, the collected reaction solution was incubated at room temperature for 1 h with 100 μL dig-300 buffer containing 2 μL hyperactive pG-Tn5 transposon. Subsequently, 300 μL tagmentation buffer was added to the collected reaction solution for fragmentation at 37°C for 1 h. The reaction was stopped by adding 2.5 μL 20 mg/mL Proteinase K, 3 μL 10% SDS, and 10 μL 0.5M EDTA at 50°C for 1 h. Lastly, DNA was extracted by phenol-chloroform and ethanol precipitation. PCR was used for the subsequent library amplification. Sequencing was performed using the Illumina Novaseq 6000 (Novogene).

Electrophoretic mobility shift assay. DNA fragments were amplified using Digoxigenin (DIG)-labeled primers as listed in Table 4. MtrA protein was phosphorylated by EnvZ (47). Next, 10 pM of purified DNA fragments were incubated using 0–5 μM MtrA or MtrA-P in binding buffer containing 5 mM Tris-HCl (pH 7.6), 50 mM KCl, 0.5 mM EDTA, 5 mM (NH₄)₂SO₄, 0.5 mM DTT, 0.1% Tween 20, 5 mM MgCl₂, and 5 mM CaCl₂ at room temperature for 30 min. The reaction was stopped with 10×loading buffer (50 mM Tris-HCl (pH 6.8), 30% glycerol, 0.12% bromophenol blue). The reaction mixtures were resolved in 5% nondenaturing polyacrylamide gels for 3 h at 40 V. Next, the DNA and proteins were transferred to nylon membranes using the semi-dry transfer method for 10 min at 10 V. For the subsequent immunological detection, DIG High Prime DNA Labeling and Detection Starter Kit I (Roche) was performed following manufacturer's instructions.

Transcriptome analysis. RNA was isolated using cells grown to the mid-exponential phase. RNA sequencing was performed using the Illumina NovaSeq6000 platform (Magigene Ltd.). Fold changes of selected genes were calculated as a ratio of treatment and control groups via fragments per transcript kilobase per million fragments mapped (FPKM) values. The differential expression analysis was performed using the DESeq2 software (81). The resulting *P*-values were adjusted using the Benjamini-Hochberg method for controlling the false discovery rate (FDR) (82). The differentially expressed genes (DEGs) were defined with a threshold of fold change ≥ 2 and false discovery rate (FDR) ≤ 0.05. Heatmaps were produced using MeV software. The KEGG Orthology (KO) assignment was obtained using the bi-directional best hit (BBH) method by the online KEGG Automatic Annotation Server (KAAS) (<http://www.genome.jp/kegg/kaas/>). Enrichment analysis of DEGs in the KEGG pathways (FDR ≤ 0.05) was performed using the OmicShare tools (www.omicshare.com/tools). The volcano plot was also produced using the OmicShare tools. Three biological replicates per condition were used in RNA-seq experiments.

Quantitative reverse transcription-PCR. The *Dietzia* cells were collected when grown to the mid-exponential phase. Total RNA from the collected cells was extracted and purified using RNAiso Plus reagent (TaKaRa). Reverse transcription was carried out using the ReverTra Ace reverse transcription kit (TOYOBO) and the random primers. The reverse transcription products (cDNA) were used as templates for real-time PCR. Relative quantities of cDNA were normalized for the 16S rRNA gene. Real-time PCR was performed using the primers listed in Table 4 with SYBR green Ex Taq kit II (TaKaRa) in the CFX9 real-time system and C1000 thermal cycler (Bio-Rad). The gene expression level was calculated by the 2^{-ΔΔCt} method (83).

TABLE 4 Primers used in this study

Primer	Sequence (5'→3')	Application	
LF	TGCTGTTGCCCCTGGACC	Δ <i>mtrAB</i> mutant strain	
LR	CCTTCATCCGTTTCCACGGTTCGTCGTCGACGACGAGGA		
RF	AAGCGTGCATAATAAGCCCTCTCGACCACTCGGAGTCCAA	Complementary plasmid	
RR	ACCGGACGGAGAGAAGGTGT		
smF	ACCGTGGAACGGATGAAGG		
smR	AGGGCTTATTATGCACGCTT		
fuF	GTCCTGCTCGACCGCTACGT		
fuR	CAGCACGGTGGCGCAGATCC		
comF	CCCAAGCTTCGACATACACGCCGACACAA		
comR	CCCAAGCTTTCACGAACGGACCTCCTCGG		
mtrAF	CCCAAGCTTCGACATACACGCCGACACAA		MtrA phosphorylation-mimic vector
mtrAR	CCCAAGCTTTCACGAGACCGGACCGGCCT		
pNVF	CCCAAGCTTGGCACTGGCCGTCG	EMSA	
pNVR	CCCAAGCTTGTGCCCGCTGAACCTCTTC		
mtrAD56EF	CCTGCTGGAGCTCATGCTCC		
mtrAD56ER	CGAGACCGGACCGGCCTTGAC		
pNVD56EF	GTACAAGGCCGGTCCGGTCTCG		
pNVD56ER	GGAGCATGAGCTCCAGCAGG		
1576DIGF	ACCCCCGACGGAACCGGT (5'-Digoxigenin)		
1576DIGR	ATGGGAAGCACTGATCACAC		
1657DIGF	GCTCTGCCAATTGAGCTAAT (5'-Digoxigenin)		
1657DIGR	TAATGGCCCCCTCCGAGCGT		
3483DIGF	CGGCCGCGGATCAGCCGAGA (5'-Digoxigenin)		
3483DIGR	AGCGCAGCCGCGGAGGGGGC		
4699DIGF	CTCTCCGATCGGGCCCCCTC (5'-Digoxigenin)		
4699DIGR	CGTTCTCCTTCGGGCCGCGG		
4713DIGF	GGAACGAGGGATTCTTCC (5'-Digoxigenin)		
4713DIGR	GGGGGAAGTATCAAGTAGTA		
5430DIGF	CGCGGTATCACCCCTCGTGG (5'-Digoxigenin)		
5430DIGR	CCGTAGACCTCCTCGACGAC	Real-time PCR	
16sRTF	GTCTCATGTTGCCAGCACGTT		
16sRTR	GCAGCCCTCTGTACTAGCCAT		
1576RTF	GGGCGAATTGCATTTCTCATC		
1576RTR	GGAGGCGGAAGTCCTGAAAG		
1657RTF	TGATCGACGTCTCCGTGGAGGA		
1657RTR	TGTA CTGCGGCTGTACCCA		
3483RTF	TGGGCTCAGGGGATCAACGA		
3483RTR	TAGCCGTCGTCGTTCAAGGT		
4699RTF	CGTCATGATCCGGTTCGACC		
4699RTR	TGCGGAAGGTGTTCTCCTGC		
4713RTF	CCTTCTGCCGTCGTCATCT		
4713RTR	TCGGCCTCGTAGTAGCGGT		
5430RTF	GGTCCTGTACGCGCTTCTGA		
5430RTR	GAACTACCGACGATCCGTC		

Moreover, the nuclease-free water in place of cDNA was used to be a negative control. All the experiments were repeated in triplicate.

Data availability. The transcriptomic raw sequence has been deposited to the National Microbiology Data Center (<https://nmdc.cn/>) under accession ID [NMDC10018150](https://nmdc.cn/resource/genomics/project/detail/NMDC10018150) (<https://nmdc.cn/resource/genomics/project/detail/NMDC10018150>).

SUPPLEMENTAL MATERIAL

Supplemental material is available online only.

SUPPLEMENTAL FILE 1, PDF file, 1.2 MB.

ACKNOWLEDGMENTS

We thank the entire Wu lab for the critical discussion of our manuscript. We thank T. Juelich (the University of Chinese Academy of Sciences, Beijing) for linguistic assistance during the preparation of this manuscript. This work was supported by National Key

R&D Program of China (2018YFA0902100 and 2021YFA0910300), and National Natural Science Foundation of China (32130004, 91951204, 32161133023, and 32170113).

REFERENCES

1. Gorla P, Plocinska R, Sarva K, Satsangi AT, Pandeeti E, Donnelly R, Dziadek J, Rajagopalan M, Madiraju MV. 2018. MtrA response regulator controls cell division and cell wall metabolism and affects susceptibility of mycobacteria to the first line antituberculosis drugs. *Front Microbiol* 9:2839. <https://doi.org/10.3389/fmicb.2018.02839>.
2. Fol M, Chauhan A, Nair NK, Maloney E, Moomey M, Jagannath C, Madiraju MV, Rajagopalan M. 2006. Modulation of *Mycobacterium tuberculosis* proliferation by MtrA, an essential two-component response regulator. *Mol Microbiol* 60:643–657. <https://doi.org/10.1111/j.1365-2958.2006.05137.x>.
3. Möker N, Brocker M, Schaffer S, Krämer R, Morbach S, Bott M. 2004. Deletion of the genes encoding the MtrA–MtrB two-component system of *Corynebacterium glutamicum* has a strong influence on cell morphology, antibiotics susceptibility and expression of genes involved in osmoprotection. *Mol Microbiol* 54:420–438. <https://doi.org/10.1111/j.1365-2958.2004.04249.x>.
4. Rahlwes KC, Sparks IL, Morita YS. 2019. Cell walls and membranes of Actinobacteria. *Bacterial Cell Walls and Membranes* 92:417–469. https://doi.org/10.1007/978-3-030-18768-2_13.
5. Wang M, Nie Y, Wu X-L. 2021. Extracellular heme recycling and sharing across species by novel mycomembrane vesicles of a Gram-positive bacterium. *ISME J* 15:605–617. <https://doi.org/10.1038/s41396-020-00800-1>.
6. Jordan S, Hutchings MI, Mascher T. 2008. Cell envelope stress response in Gram-positive bacteria. *FEMS Microbiol Rev* 32:107–146. <https://doi.org/10.1111/j.1574-6976.2007.00091.x>.
7. Mitchell AM, Silhavy TJ. 2019. Envelope stress responses: balancing damage repair and toxicity. *Nat Rev Microbiol* 17:417–428. <https://doi.org/10.1038/s41579-019-0199-0>.
8. Mike LA, Choby JE, Brinkman PR, Olive LQ, Dutter BF, Ivan SJ, Gibbs CM, Sulikowski GA, Stauff DL, Skaar EP. 2014. Two-component system cross-regulation integrates *Bacillus anthracis* response to heme and cell envelope stress. *PLoS Pathog* 10:e1004044. <https://doi.org/10.1371/journal.ppat.1004044>.
9. Nielsen PK, Andersen AZ, Mols M, van der Veen S, Abee T, Kallipolitis BH. 2012. Genome-wide transcriptional profiling of the cell envelope stress response and the role of LisRK and CesRK in *Listeria monocytogenes*. *Microbiology (Reading)* 158:963–974. <https://doi.org/10.1099/mic.0.055467-0>.
10. Jubelin G, Vianney A, Beloin C, Ghigo J-M, Lazzaroni J-C, Lejeune P, Dorel C. 2005. CpxR/OmpR interplay regulates curli gene expression in response to osmolarity in *Escherichia coli*. *J Bacteriol* 187:2038–2049. <https://doi.org/10.1128/JB.187.6.2038-2049.2005>.
11. Danese PN, Silhavy TJ. 1998. CpxP, a stress-combative member of the Cpx regulon. *J Bacteriol* 180:831–839. <https://doi.org/10.1128/JB.180.4.831-839.1998>.
12. Price NL, Raivio TL. 2009. Characterization of the Cpx regulon in *Escherichia coli* strain MC4100. *J Bacteriol* 191:1798–1815. <https://doi.org/10.1128/JB.00798-08>.
13. Raivio TL, Leblanc SK, Price NL. 2013. The *Escherichia coli* Cpx envelope stress response regulates genes of diverse function that impact antibiotic resistance and membrane integrity. *J Bacteriol* 195:2755–2767. <https://doi.org/10.1128/JB.00105-13>.
14. Meng J, Young G, Chen J. 2021. The Rcs system in Enterobacteriaceae: envelope stress responses and virulence regulation. *Front Microbiol* 12:627104. <https://doi.org/10.3389/fmicb.2021.627104>.
15. Bury-Moné S, Nomane Y, Raymond N, Barbet R, Jacquet E, Imbeaud S, Jacq A, Bouloc P. 2009. Global analysis of extracytoplasmic stress signaling in *Escherichia coli*. *PLoS Genet* 5:e1000651. <https://doi.org/10.1371/journal.pgen.1000651>.
16. Clarke DJ. 2010. The Rcs phosphorelay: more than just a two-component pathway. *Future Microbiol* 5:1173–1184. <https://doi.org/10.2217/fmb.10.83>.
17. Dubrac S, Bisicchia P, Devine KM, Msadek T. 2008. A matter of life and death: cell wall homeostasis and the WalkR (YycGF) essential signal transduction pathway. *Mol Microbiol* 70:1307–1322. <https://doi.org/10.1111/j.1365-2958.2008.06483.x>.
18. Dubrac S, Msadek T. 2008. Tearing down the wall: peptidoglycan metabolism and the Walk/WalR (YycG/YycF) essential two-component system pp 214–228. In Utsumi R (ed), *Bacterial signal transduction: networks and drug targets*. Advances in Experimental Medicine and Biology, vol 631. Springer, New York, NY. https://doi.org/10.1007/978-0-387-78885-2_15.
19. Dörr T, Alvarez L, Delgado F, Davis BM, Cava F, Waldor MK. 2016. A cell wall damage response mediated by a sensor kinase/response regulator pair enables beta-lactam tolerance. *Proc Natl Acad Sci U S A* 113:404–409. <https://doi.org/10.1073/pnas.1520333113>.
20. Purushotham G, Sarva KB, Blaszczyk E, Rajagopalan M, Madiraju MV. 2015. *Mycobacterium tuberculosis* oriC sequestration by MtrA response regulator. *Mol Microbiol* 98:586–604. <https://doi.org/10.1111/mmi.13144>.
21. Banerjee SK, Lata S, Sharma AK, Bagchi S, Kumar M, Sahu SK, Sarkar D, Gupta P, Jana K, Gupta UD, Singh R, Saha S, Basu J, Kundu M. 2019. The sensor kinase MtrB of *Mycobacterium tuberculosis* regulates hypoxic survival and establishment of infection. *J Biol Chem* 294:19862–19876. <https://doi.org/10.1074/jbc.RA119.009449>.
22. Plocinska R, Martinez L, Gorla P, Pandeeti E, Sarva K, Blaszczyk E, Dziadek J, Madiraju MV, Rajagopalan M. 2014. *Mycobacterium tuberculosis* MtrB sensor kinase interactions with FtsI and Wag31 proteins reveal a role for MtrB distinct from that regulating MtrA activities. *J Bacteriol* 196:4120–4129. <https://doi.org/10.1128/JB.01795-14>.
23. Brocker M, Mack C, Bott M. 2011. Target genes, consensus binding site, and role of phosphorylation for the response regulator MtrA of *Corynebacterium glutamicum*. *J Bacteriol* 193:1237–1249. <https://doi.org/10.1128/JB.01032-10>.
24. Plocinska R, Purushotham G, Sarva K, Vadrevu IS, Pandeeti EV, Arora N, Plocinski P, Madiraju MV, Rajagopalan M. 2012. Septal localization of the *Mycobacterium tuberculosis* MtrB sensor kinase promotes MtrA regulon expression. *J Biol Chem* 287:23887–23899. <https://doi.org/10.1074/jbc.M112.346544>.
25. Duckworth AW, Grant S, Grant WD, Jones BE, Meijer D. 1998. *Dietzia natronolimnaios* sp. nov., a new member of the genus *Dietzia* isolated from an East African soda lake. *Extremophiles* 2:359–366. <https://doi.org/10.1007/s007920050079>.
26. Borsodi A, Micsinai A, Rusznyák A, Vladár P, Kovacs G, Toth E, Marialigeti K. 2005. Diversity of alkaliphilic and alkalitolerant bacteria cultivated from decomposing reed rhizomes in a Hungarian soda lake. *Microb Ecol* 50:9–18. <https://doi.org/10.1007/s00248-004-0063-1>.
27. Maldonado LA, Fragoso-Yañez D, Pérez-García A, Rosellón-Druker J, Quintana ET. 2009. Actinobacterial diversity from marine sediments collected in Mexico. *Antonie Van Leeuwenhoek* 95:111–120. <https://doi.org/10.1007/s10482-008-9294-3>.
28. Wang W, Cai B, Shao Z. 2014. Oil degradation and biosurfactant production by the deep sea bacterium *Dietzia maris* As-13-3. *Front Microbiol* 5:711. <https://doi.org/10.3389/fmicb.2014.00711>.
29. Mayilraj S, Suresh K, Kroppenstedt R, Saini H. 2006. *Dietzia kunjamsensis* sp. nov., isolated from the Indian Himalayas. *Int J Syst Evol Microbiol* 56:1667–1671. <https://doi.org/10.1099/ijs.0.64212-0>.
30. Li J, Chen C, Zhao G-Z, Klenk H-P, Pukall R, Zhang Y-Q, Tang S-K, Li W-J. 2009. Description of *Dietzia lutea* sp. nov., isolated from a desert soil in Egypt. *Syst Appl Microbiol* 32:118–123. <https://doi.org/10.1016/j.syapm.2008.11.007>.
31. Borzenkov I, Milekhina E, Gotoeva M, Rozanova E, Belyaev S. 2006. The properties of hydrocarbon-oxidizing bacteria isolated from the oilfields of Tatarstan, Western Siberia, and Vietnam. *Microbiology* 75:66–72. <https://doi.org/10.1134/S0026261706010127>.
32. Wang X-B, Chi C-Q, Nie Y, Tang Y-Q, Tan Y, Wu G, Wu X-L. 2011. Degradation of petroleum hydrocarbons (C6–C40) and crude oil by a novel *Dietzia* strain. *Bioresour Technol* 102:7755–7761. <https://doi.org/10.1016/j.biortech.2011.06.009>.
33. Li J, Zhao G-Z, Zhang Y-Q, Klenk H-P, Pukall R, Qin S, Xu L-H, Li W-J. 2008. *Dietzia schimae* sp. nov. and *Dietzia cercidiphylli* sp. nov., from surface-sterilized plant tissues. *Int J Syst Evol Microbiol* 58:2549–2554. <https://doi.org/10.1099/ijs.0.2008/000919-0>.
34. Dekio I, Sakamoto M, Hayashi H, Amagai M, Suematsu M, Benno Y. 2007. Characterization of skin microbiota in patients with atopic dermatitis and in normal subjects using 16S rRNA gene-based comprehensive analysis. *J Med Microbiol* 56:1675–1683. <https://doi.org/10.1099/jmm.0.47268-0>.
35. Jones AL, Koerner RJ, Natarajan S, Perry JD, Goodfellow M. 2008. *Dietzia papillomatosis* sp. nov., a novel actinomycete isolated from the skin of an immunocompetent patient with confluent and reticulated papillomatosis. *Int J Syst Evol Microbiol* 58:68–72. <https://doi.org/10.1099/ijs.0.65178-0>.
36. Koerner RJ, Goodfellow M, Jones AL. 2009. The genus *Dietzia*: a new home for some known and emerging opportunist pathogens. *FEMS*

- Immunol Med Microbiol 55:296–305. <https://doi.org/10.1111/j.1574-695X.2008.00513.x>.
37. Pidoux O, Argenson J-N, Jacomo V, Drancourt M. 2001. Molecular identification of a *Dietzia maris* hip prosthesis infection isolate. J Clin Microbiol 39:2634–2636. <https://doi.org/10.1128/JCM.39.7.2634-2636.2001>.
 38. Bemer-Melchior P, Haloun A, Riegel P, Drugeon H. 1999. Bacteremia due to *Dietzia maris* in an immunocompromised patient. Clin Infect Dis 29:1338–1340. <https://doi.org/10.1086/313490>.
 39. Yassin A, Hupfer H, Schaal K. 2006. *Dietzia cinnamea* sp. nov., a novel species isolated from a perianal swab of a patient with a bone marrow transplant. Int J Syst Evol Microbiol 56:641–645. <https://doi.org/10.1099/ijso.0.63863-0>.
 40. Gharibzadeh SMT, Razavi SH, Mousavi SM. 2014. Characterization of bacteria of the genus *Dietzia*: an updated review. Ann Microbiol 64:1–11. <https://doi.org/10.1007/s13213-013-0603-3>.
 41. Chen W, Li J, Sun X, Min J, Hu X. 2017. High efficiency degradation of alkanes and crude oil by a salt-tolerant bacterium *Dietzia* species CN-3. International Biodeterioration & Biodegradation 118:110–118. <https://doi.org/10.1016/j.ibiod.2017.01.029>.
 42. Fang H, Xu JB, Nie Y, Wu XL. 2021. Pan-genomic analysis reveals that the evolution of *Dietzia* species depends on their living habitats. Environ Microbiol 23:861–877. <https://doi.org/10.1111/1462-2920.15176>.
 43. Click RE, Van Kampen CL. 2010. Assessment of *Dietzia* subsp. C79793-74 for treatment of cattle with evidence of paratuberculosis. Virulence 1:145–155. <https://doi.org/10.4161/viru.1.3.10897>.
 44. Click RE. 2015. Crohn's disease therapy with *Dietzia*: the end of anti-inflammatory drugs. Future Microbiol 10:147–150. <https://doi.org/10.2217/fmb.14.133>.
 45. Szvetnik A, Bihari Z, Szabo Z, Kelemen O, Kiss I. 2010. Genetic manipulation tools for *Dietzia* spp. J Appl Microbiol 109:1845–1852. <https://doi.org/10.1111/j.1365-2672.2010.04818.x>.
 46. Kaya-Okur HS, Wu SJ, Codomo CA, Pledger ES, Bryson TD, Henikoff JG, Ahmad K, Henikoff S. 2019. CUT&Tag for efficient epigenomic profiling of small samples and single cells. Nat Commun 10:1–10. <https://doi.org/10.1038/s41467-019-09982-5>.
 47. Al Zayer M, Stankowska D, Dziedzic R, Sarva K, Madiraju MV, Rajagopalan M. 2011. *Mycobacterium tuberculosis* mtrA merodiploid strains with point mutations in the signal-receiving domain of MtrA exhibit growth defects in nutrient broth. Plasmid 65:210–218. <https://doi.org/10.1016/j.plasmid.2011.01.002>.
 48. Bailey TL, Boden M, Buske FA, Frith M, Grant CE, Clementi L, Ren J, Li WW, Noble WS. 2009. MEME SUITE: tools for motif discovery and searching. Nucleic Acids Res 37:W202–W208. <https://doi.org/10.1093/nar/gkp335>.
 49. Dajkovic A, Tesson B, Chauhan S, Courtin P, Keary R, Flores P, Marliere C, Filipe SR, Chapot-Chartier MP, Carballido-Lopez R. 2017. Hydrolysis of peptidoglycan is modulated by amidation of meso-diaminopimelic acid and Mg²⁺ in *Bacillus subtilis*. Mol Microbiol 104:972–988. <https://doi.org/10.1111/mmi.13673>.
 50. Chen S, Wu Y, Niu H, Sun J, Han X, Zhang L. 2021. Imbalance between peptidoglycan synthases and hydrolases regulated lysis of *Lactobacillus bulgaricus* in batch culture. Arch Microbiol 203:4571–4578. <https://doi.org/10.1007/s00203-021-02433-0>.
 51. Brunet YR, Wang X, Rudner DZ. 2019. SweC and SweD are essential co-factors of the FtsEX-CwlO cell wall hydrolase complex in *Bacillus subtilis*. PLoS Genet 15:e1008296. <https://doi.org/10.1371/journal.pgen.1008296>.
 52. Rozwarski DA, Grant GA, Barton DH, Jacobs WR, Sacchettini JC. 1998. Modification of the NADH of the isoniazid target (InhA) from *Mycobacterium tuberculosis*. Science 279:98–102. <https://doi.org/10.1126/science.279.5347.98>.
 53. Belanger AE, Besra GS, Ford ME, Mikusová K, Belisle JT, Brennan PJ, Inamine JM. 1996. The *embAB* genes of *Mycobacterium avium* encode an arabinosyl transferase involved in cell wall arabinan biosynthesis that is the target for the antimycobacterial drug ethambutol. Proc Natl Acad Sci U S A 93:11919–11924. <https://doi.org/10.1073/pnas.93.21.11919>.
 54. Nagai K, Davies TA, Jacobs MR, Appelbaum PC. 2002. Effects of amino acid alterations in penicillin-binding proteins (PBPs) 1a, 2b, and 2x on PBP affinities of penicillin, ampicillin, amoxicillin, cefditoren, cefuroxime, cefprozil, and cefaclor in 18 clinical isolates of penicillin-susceptible, intermediate, and-resistant pneumococci. Antimicrob Agents Chemother 46:1273–1280. <https://doi.org/10.1128/AAC.46.5.1273-1280.2002>.
 55. Georgopadakou NH, Dix BA, Mauriz YR. 1986. Possible physiological functions of penicillin-binding proteins in *Staphylococcus aureus*. Antimicrob Agents Chemother 29:333–336. <https://doi.org/10.1128/AAC.29.2.333>.
 56. Loll PJ, Axelsen PH. 2000. The structural biology of molecular recognition by vancomycin. Annu Rev Biophys Biomol Struct 29:265–289. <https://doi.org/10.1146/annurev.biophys.29.1.265>.
 57. Hiramatsu K. 2001. Vancomycin-resistant *Staphylococcus aureus*: a new model of antibiotic resistance. Lancet Infect Dis 1:147–155. [https://doi.org/10.1016/S1473-3099\(01\)00091-3](https://doi.org/10.1016/S1473-3099(01)00091-3).
 58. Hanaki H, Labischinski H, Inaba Y, Kondo N, Murakami H, Hiramatsu K. 1998. Increase in glutamine-non-amidated mucopeptides in the peptidoglycan of vancomycin-resistant *Staphylococcus aureus* strain Mu50. J Antimicrob Chemother 42:315–320. <https://doi.org/10.1093/jac/42.3.315>.
 59. Raivio TL. 2014. Everything old is new again: an update on current research on the Cpx envelope stress response. Biochim Biophys Acta 1843:1529–1541. <https://doi.org/10.1016/j.bbamcr.2013.10.018>.
 60. Konovalova A, Perlman DH, Cowles CE, Silhavy TJ. 2014. Transmembrane domain of surface-exposed outer membrane lipoprotein RcsF is threaded through the lumen of β -barrel proteins. Proc Natl Acad Sci U S A 111:E4350–E4358. <https://doi.org/10.1073/pnas.1417138111>.
 61. Konovalova A, Mitchell AM, Silhavy TJ. 2016. A lipoprotein/ β -barrel complex monitors lipopolysaccharide integrity transducing information across the outer membrane. Elife 5:e15276. <https://doi.org/10.7554/eLife.15276>.
 62. Cho S-H, Szewczyk J, Pesavento C, Zietek M, Banzhaf M, Roszczzenko P, Asmar A, Laloux G, Hov A-K, Leverrier P, Van der Henst C, Vertommen D, Typas A, Collet J-F. 2014. Detecting envelope stress by monitoring β -barrel assembly. Cell 159:1652–1664. <https://doi.org/10.1016/j.cell.2014.11.045>.
 63. Flores-Kim J, Darwin AJ. 2014. Regulation of bacterial virulence gene expression by cell envelope stress responses. Virulence 5:835–851. <https://doi.org/10.4161/21505594.2014.965580>.
 64. Barthe P, Mukamolova GV, Roumestand C, Cohen-Gonsaud M. 2010. The structure of PknB extracellular PASTA domain from *Mycobacterium tuberculosis* suggests a ligand-dependent kinase activation. Structure 18:606–615. <https://doi.org/10.1016/j.str.2010.02.013>.
 65. Wang Q, Marchetti R, Priscic S, Ishii K, Arai Y, Ohta I, Inuki S, Uchiyama S, Silipo A, Molinaro A, Husson RN, Fukase K, Fujimoto Y. 2017. A comprehensive study of the interaction between peptidoglycan fragments and the extracellular domain of *Mycobacterium tuberculosis* Ser/Thr kinase PknB. Chembiochem 18:2094–2098. <https://doi.org/10.1002/cbic.201700385>.
 66. Shah IM, Laaberki M-H, Popham DL, Dworkin J. 2008. A eukaryotic-like Ser/Thr kinase signals bacteria to exit dormancy in response to peptidoglycan fragments. Cell 135:486–496. <https://doi.org/10.1016/j.cell.2008.08.039>.
 67. Mueller EA, Egan AJ, Breukink E, Vollmer W, Levin PA. 2019. Plasticity of *Escherichia coli* cell wall metabolism promotes fitness and antibiotic resistance across environmental conditions. Elife 8:e40754. <https://doi.org/10.7554/eLife.40754>.
 68. Mueller EA, Levin PA. 2020. Bacterial cell wall quality control during environmental stress. mBio 11:e02456-20. <https://doi.org/10.1128/mBio.02456-20>.
 69. Jollès P, Jollès J. 1984. What's new in lysozyme research? Mol Cell Biochem 63:165–189.
 70. Mainardi J-L, Fourgeaud M, Hugonnet J-E, Dubost L, Brouard J-P, Ouazzani J, Rice LB, Gutmann L, Arthur M. 2005. A novel peptidoglycan cross-linking enzyme for a β -lactam-resistant transpeptidation pathway. J Biol Chem 280:38146–38152. <https://doi.org/10.1074/jbc.M507384200>.
 71. Baranowski C, Welsh MA, Sham L-T, Eskandarian HA, Lim HC, Kieser KJ, Wagner JC, McKinney JD, Fantner GE, Ioerger TR, Walker S, Bernhardt TG, Rubin EJ, Rego EH. 2018. Maturing *Mycobacterium smegmatis* peptidoglycan requires non-canonical crosslinks to maintain shape. Elife 7:e37516. <https://doi.org/10.7554/eLife.37516>.
 72. Magnet S, Bellais S, Dubost L, Fourgeaud M, Mainardi J-L, Petit-Frère S, Marie A, Mengin-Lecreux D, Arthur M, Gutmann L. 2007. Identification of the L, D-transpeptidases responsible for attachment of the Braun lipoprotein to *Escherichia coli* peptidoglycan. J Bacteriol 189:3927–3931. <https://doi.org/10.1128/JB.00084-07>.
 73. Thompson JD, Higgins DG, Gibson TJ. 1994. CLUSTAL W: improving the sensitivity of progressive multiple sequence alignment through sequence weighting, position-specific gap penalties and weight matrix choice. Nucleic Acids Res 22:4673–4680. <https://doi.org/10.1093/nar/22.22.4673>.
 74. Saitou N, Nei M. 1987. The neighbor-joining method: a new method for reconstructing phylogenetic trees. Mol Biol Evol 4:406–425. <https://doi.org/10.1093/oxfordjournals.molbev.a040454>.
 75. Kumar S, Tamura K, Nei M. 1994. MEGA: molecular evolutionary genetics analysis software for microcomputers. Comput Appl Biosci 10:189–191. <https://doi.org/10.1093/bioinformatics/10.2.189>.
 76. Fang H, Qin X-Y, Zhang K-D, Nie Y, Wu X-L. 2018. Role of the Group 2 Mrp sodium/proton antiporter in rapid response to high alkaline shock in the

- alkaline-and salt-tolerant *Dietzia* sp. DQ12-45-1b. Appl Microbiol Biotechnol 102:3765–3777. <https://doi.org/10.1007/s00253-018-8846-3>.
77. Van Kessel JC, Hatfull GF. 2007. Recombineering in *Mycobacterium tuberculosis*. Nat Methods 4:147–152. <https://doi.org/10.1038/nmeth996>.
 78. Lu S, Nie Y, Tang Y-Q, Xiong G, Wu X-L. 2014. A critical combination of operating parameters can significantly increase the electrotransformation efficiency of a Gram-positive *Dietzia* strain. J Microbiol Methods 103: 144–151. <https://doi.org/10.1016/j.mimet.2014.05.015>.
 79. Botella H, Vaubourgeix J, Lee MH, Song N, Xu W, Makinoshima H, Glickman MS, Ehrt S. 2017. *Mycobacterium tuberculosis* protease MarP activates a peptidoglycan hydrolase during acid stress. EMBO J 36: 536–548. <https://doi.org/10.15252/emj.201695028>.
 80. Alqaisi MR, Mohsin RM, Ahmed TS. 2020. Efficiency of image analysis as a direct method in spore dimensions measurement. Plant Cell Biotechnology and Molecular Biology 21:57–64.
 81. Varet H, Brillet-Guéguen L, Coppée J-Y, Dillies M-A. 2016. SARTools: a DESeq2- and EdgeR-based R pipeline for comprehensive differential analysis of RNA-Seq data. PLoS One 11:e0157022. <https://doi.org/10.1371/journal.pone.0157022>.
 82. Benjamini Y, Hochberg Y. 1995. Controlling the false discovery rate: a practical and powerful approach to multiple testing. J R Stat Soc: Series B (Methodological) 57:289–300. <https://doi.org/10.1111/j.2517-6161.1995.tb02031.x>.
 83. Livak KJ, Schmittgen TD. 2001. Analysis of relative gene expression data using real-time quantitative PCR and the $2^{-\Delta\Delta CT}$ method. Methods 25: 402–408. <https://doi.org/10.1006/meth.2001.1262>.